

Article

A Nation-by-Nation Assessment of the Contribution of Southeast Asian Open Biomass Burning to PM_{2.5} in Thailand Using the Community Multiscale Air Quality-Integrated Source Apportionment Method Model

Nanthapong Chantaraprachoom ^{1,*} , Hikari Shimadera ¹ , Katsushige Uranishi ² , Luong Viet Mui ¹ , Tomohito Matsuo ¹  and Akira Kondo ¹ 

¹ Graduate School of Engineering, Osaka University, 2-1 Yamadaoka, Suita, Osaka 565-0871, Japan; shimadera@see.eng.osaka-u.ac.jp (H.S.); luong-vm@ea.see.eng.osaka-u.ac.jp (L.V.M.); matsuo@see.eng.osaka-u.ac.jp (T.M.); kondo@see.eng.osaka-u.ac.jp (A.K.)

² Department of Life and Environment Engineering, The University of Kitakyushu, 1-1 Hibikino, Wakamatsu-ku, Kitakyushu, Fukuoka 808-0135, Japan; uranishi@kitakyu-u.ac.jp

* Correspondence: nanthapongc@ea.see.eng.osaka-u.ac.jp

Abstract: This study utilized the Community Multiscale Air Quality (CMAQ) model to assess the impact of open biomass burning (OBB) in Thailand and neighboring countries—Myanmar, Laos, Cambodia, and Vietnam—on the PM_{2.5} concentrations in the Bangkok Metropolitan Region (BMR) and Upper Northern Region of Thailand. The Upper Northern Region was further divided into the west, central, and east sub-regions (WUN, CUN, and EUN) based on geographical borders. The CMAQ model was used to simulate the spatiotemporal variations in PM_{2.5} over a wide domain in Asia in 2019. The Integrated Source Apportionment Method (ISAM) was utilized to quantify the contributions from OBB from each country. The results showed that OBB had a minor impact on PM_{2.5} in the BMR, but transboundary transport from Myanmar contributed to an increase in PM_{2.5} levels during the peak burning period from March to April. In contrast, OBB substantially impacted PM_{2.5} in the Upper Northern Region, with Myanmar being the major contributor in WUN and CUN and domestic burning being the major contributor to EUN during the peak months. Despite Laos having the highest OBB emissions, meteorological conditions caused the spread of PM_{2.5} eastward rather than into Thailand. These findings highlight the critical impact of regional transboundary transport and emphasize the necessity for collaborative strategies for mitigating PM_{2.5} pollution across Southeast Asia.

Keywords: air pollution; particulate matter; open biomass burning; transboundary transport; air quality simulation; source apportionment; Northern Thailand; Bangkok Metropolitan Region



Citation: Chantaraprachoom, N.; Shimadera, H.; Uranishi, K.; Mui, L.V.; Matsuo, T.; Kondo, A. A Nation-by-Nation Assessment of the Contribution of Southeast Asian Open Biomass Burning to PM_{2.5} in Thailand Using the Community Multiscale Air Quality-Integrated Source Apportionment Method Model. *Atmosphere* **2024**, *15*, 1358. <https://doi.org/10.3390/atmos15111358>

Academic Editors: Evgueni Kassianov, Manish Shrivastava, Manvendra Dubey and Arthur J. Sedlacek

Received: 4 October 2024

Revised: 30 October 2024

Accepted: 4 November 2024

Published: 12 November 2024



Copyright: © 2024 by the authors. Licensee MDPI, Basel, Switzerland. This article is an open access article distributed under the terms and conditions of the Creative Commons Attribution (CC BY) license (<https://creativecommons.org/licenses/by/4.0/>).

1. Introduction

Open biomass burning (OBB) of agricultural residues is extensively practiced by farmers across Southeast Asian countries [1–4]. This practice is favored primarily due to its cost-effectiveness in swiftly clearing agricultural waste, pests, and unwanted or diseased crops from fields, facilitating faster crop rotation while also replenishing the nutrients in the soil [4–7]. Despite these benefits, fumes and particulate pollutants emitted from OBB significantly degrade ambient air quality and pose risks to human health [8–12]. Some of the major pollutants produced during this practice are particulate pollutants with diameters smaller than 2.5 μm (PM_{2.5}) [13–15]. These tiny particles are known to pose risks to human health, as they can penetrate deep into the lungs and even enter the bloodstream, leading to respiratory and cardiovascular diseases [16–18]. Moreover, PM_{2.5} not only contributes to local air pollution but also to regional air pollution. Due to their small size, particulate pollutants resulting from OBB can remain airborne for extended periods and travel long

distances under favorable conditions, thus causing transboundary transport [3,11,12,19,20]. Furthermore, PM_{2.5} also has a considerable impact on global climate change. Due to their ability to interact with solar radiation, these particles can alter atmospheric temperature dynamics by absorbing or scattering sunlight, leading to changes in cloud formation, atmospheric circulation, and precipitation patterns [21–25].

PM_{2.5} from both domestic and transboundary OBB sources has been a persistent issue in Thailand, especially in the Upper Northern Region during the intensive burning season at the end of the dry season, which spans from January to April [26–30]. According to a report from the Pollution Control Department (PCD) [26], the annual national average PM_{2.5} concentration in Thailand has consistently exceeded the recommended value from the World Health Organization's air quality guidelines [31] by five times in the last decade. The high daily concentrations of PM_{2.5} have been reported to be associated with increases in hospitalization and mortality rates in major cities in Thailand [15,30,32–35]. Furthermore, research findings also suggest that Thailand's economy is negatively impacted by PM_{2.5} pollution. For instance, Linh Thao et al. estimated that PM_{2.5} pollution cost Thailand's economy USD 1.19 billion in 2012. In addition, increased daily concentrations of PM_{2.5} have been linked to a decline in tourism [36–38].

Numerous studies have examined the contribution of OBB to PM_{2.5} pollution in Thailand and Southeast Asia as a whole. Yin et al. [13] assessed the distribution of OBB and its effects on ambient air quality in mainland Southeast Asia over a 15-year period from 2001 to 2016. Their findings indicated that OBB is the largest contributor to the annual average PM_{2.5} concentration in mainland Southeast Asia, contributing to almost half of all PM_{2.5}. Hassan Bran et al. [39] utilized the WRF-Chem atmospheric chemical transport model to conduct a source apportionment of PM_{2.5} in Thailand in 2017 and 2019. Their findings revealed that OBB was the primary source of PM_{2.5} in Thailand, contributing 34.3% and 47.4% of the annual PM_{2.5} concentrations in 2017 and 2019, respectively. Song et al. [40] performed source apportionment using radiocarbon analysis on PM_{2.5} samples collected in urban and rural areas of Chiang Mai, a province in Upper Northern Thailand. The source apportionment results revealed that most PM_{2.5} in both urban and rural areas of Upper Northern Thailand was from OBB. Chansuebsri et al. [41] conducted a similar source apportionment using the positive matrix factorization (PMF) receptor model and the potential source contribution function (PSCF). The PMF results showed that biomass burning contributed up to half of the PM_{2.5} in Chiang Mai during a high burning episode, while the PSCF results further revealed that the area along the border between Thailand and Myanmar was potentially the main source area of OBB. Amnuaylojaroen et al. [27] employed an atmospheric chemical transport model alongside satellite data to investigate the potential contribution of transboundary transport to PM_{2.5} pollution in Northern Thailand during periods of intense burning. The results indicated that biomass burning from neighboring countries had a greater potential to contribute to air pollution in Northern Thailand than domestic emissions. Similarly, Inlaung et al. [20] reported that transboundary transport significantly contributed to PM_{2.5} in Northern Thailand, often surpassing the contributions from domestic burning.

Despite the clear link between OBB and PM_{2.5} pollution in Thailand, it remains unclear whether domestic burning or transboundary transport contributes more significantly to the problem. Furthermore, the specific contributions of individual neighboring countries to PM_{2.5} in Thailand have not been thoroughly investigated. This uncertainty complicates the development of effective mitigation strategies, as policymakers may need to deploy different measures depending on whether the primary source of pollution is local or originates from other countries. In addition, the lack of research addressing the specific contributions from each country makes it more challenging to coordinate regional efforts to effectively address the issue. To address this knowledge gap, this study aims to assess the contribution of OBB to PM_{2.5} in Thailand on a nation-by-nation basis using an atmospheric chemical transport model.

2. Materials and Methods

2.1. Study Area

This study assesses the contributions of OBB from target source countries to two key receptor areas in Thailand: the Upper Northern Region and the Bangkok Metropolitan Region (BMR). The target source countries include Thailand, Laos, Myanmar, Cambodia, and Vietnam. To comprehensively capture the dispersion of $PM_{2.5}$ from these target source countries, the modeling domain for this study was set to cover a wide area of Asia, including Southeast Asia, India, parts of China, and the southwestern Pacific region, as illustrated in Figure 1a. The locations of the target source countries, the Upper Northern Region, and the BMR are shown in Figure 1b–d, respectively.

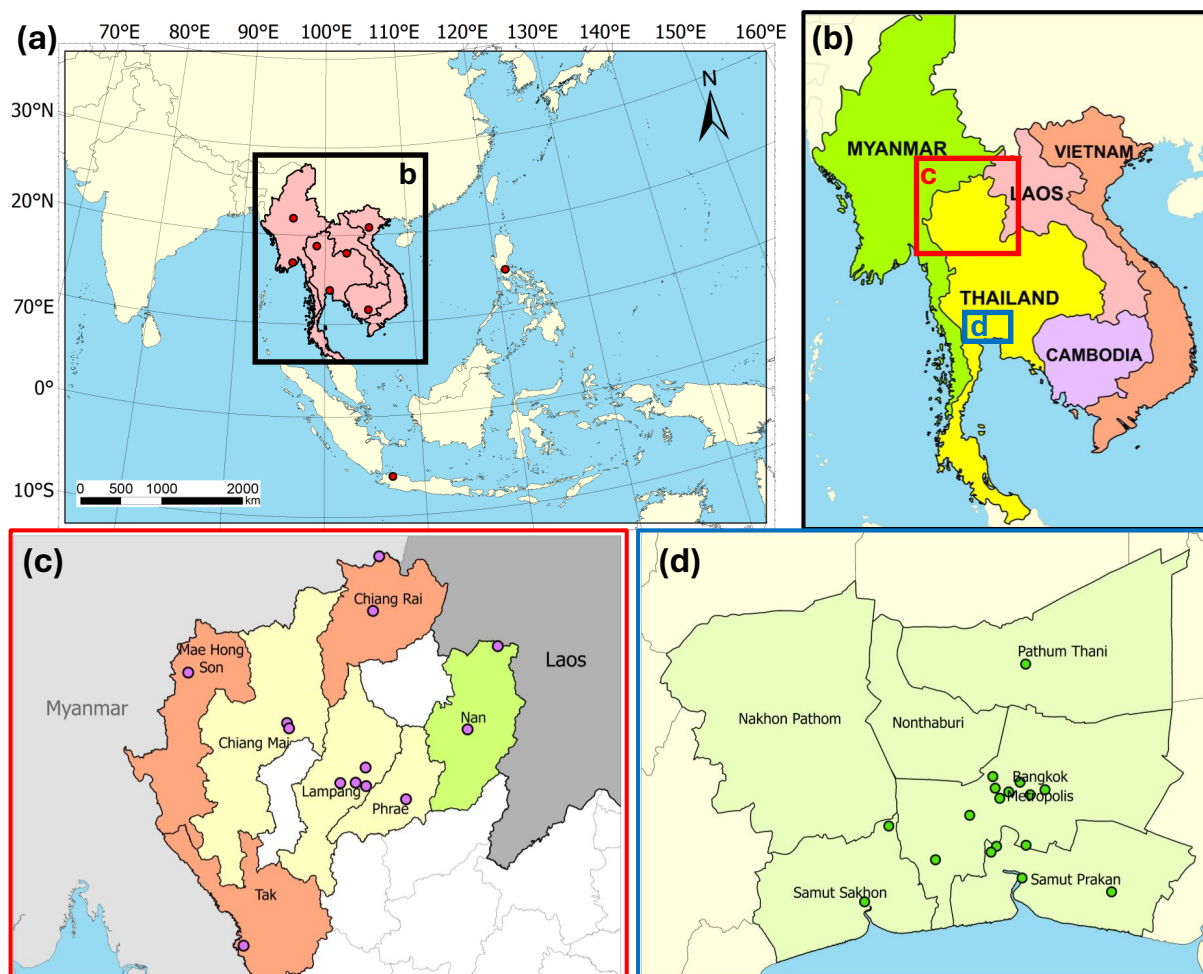


Figure 1. Study area: (a) Modeling domain. The locations of EANET monitoring stations used in the model evaluation are marked with red circles. (b) Target source countries. (c) Upper Northern Region of Thailand. The locations of PCD monitoring stations used in the model evaluation are shown in purple circles. (d) BMR, with the locations of PCD monitoring stations marked with green circles.

The Upper Northern Region of Thailand was selected due to its significant $PM_{2.5}$ pollution issues. According to a report from the Pollution Control Department [42], eight provinces in Upper Northern Thailand, namely, Mae Hong Son, Chiang Mai, Chiang Rai, Lamphun, Lamphun, Phrae, Nan, and Tak, experience severe $PM_{2.5}$ episodes in which the national standard level is exceeded for more than 30 days each year. Due to its topography, this region is particularly vulnerable to $PM_{2.5}$ pollution. As it is surrounded by high mountainous terrain combined with peculiar meteorological features, such as calm winds and temperature inversion, the Upper Northern Region is prone to air stagnation, leading to the accumulation of air pollutants [43]. This is particularly true during the dry season, in which the level of burning activities in this region and in bordering countries is high [44]. As

PM_{2.5} from transboundary transport is expected to be more severe in areas closer to border provinces [20], the Upper Northern Region was further divided into three sub-areas in this study: the West Upper Northern (WUN), Central Upper Northern (CUN), and East Upper Northern (EUN) sub-areas. These sub-areas were defined based on their geographical borders. The WUN includes Mae Hong Son, Tak, and Chiang Rai, which are adjacent to Myanmar. The CUN includes Chiang Mai, Lampang, and Phrae, which are inland and do not border any countries, consisting mainly of urban areas. Lastly, EUN covers Nan, which borders Laos. Lamphun was excluded from this study due to insufficient PM_{2.5} observation data for the study period. This lack of data made it impossible to validate the model accurately in this region, which could lead to uncertain results in source apportionment.

BMR was included as a target receptor area due to its demographic and economic significance. The BMR comprises Bangkok (the capital of Thailand) and its vicinity. It consists of six provinces: Bangkok, Nakhon Pathom, Pathum Thani, Nonthaburi, Samut Prakan, and Samut Sakhon. It is the most densely populated region of Thailand, housing 16% of the nation's population [45]. As the most populated area in Thailand, the adverse health impacts of PM_{2.5} pollution can affect a large number of residents, making it crucial to understand the sources and mitigation strategies for this pollutant.

2.2. Model Configuration

In this study, the Community Multiscale Air Quality (CMAQ) model version 5.3.3 [46] was used to simulate the spatiotemporal variations in PM_{2.5} in the modeling domain. The horizontal grid resolution of the domain was 45 × 45 km, and the number of grid cells was 192 × 129. The simulation period was from January to December 2019, with December 2018 as a spin-up period. The year 2019 was chosen as the study period because it was the most recent typical year prior to the COVID-19 pandemic, during which there were significantly fewer anthropogenic emissions due to lockdown measures [47,48]. The chemical mechanism developed by the State Air Pollution Research Center (SAPRC) (version 07TC) [49] and the *aero6* aerosol module with aqueous chemistry were employed. The boundary conditions used were derived from the output of the Whole Atmosphere Community Climate Model (WACCM) [50].

The meteorological field input for the CMAQ-ISAM model was generated using the Weather Research and Forecasting (WRF) model version 4.3 [51]. The following physics and dynamics options were employed for WRF simulation: the Morrison double-moment microphysics scheme [52], the Rapid Radiative Transfer Model for Global Climate Models [53] for longwave and shortwave radiation, the MYNN surface layer scheme [54], the Noah land surface model [55], the MYNN3 planetary boundary layer (PBL) scheme [56], and the Grell 3D ensemble cumulus scheme [57]. The topology and land use data used were global multi-resolution terrain elevation data (GMTED) from 2010 [58] and moderate-resolution imaging spectroradiometer (MODIS) data [59], respectively. Grid nudging was applied throughout the entire simulation, using nudging coefficients of $1.0 \times 10^{-4} \text{ s}^{-1}$ for the wind components and $5.0 \times 10^{-4} \text{ s}^{-1}$ for both potential temperature and the water vapor mixing ratio. The initial and boundary conditions for the WRF model were obtained from ECMWF Reanalysis version 5 (ERA5) [60]. The hourly results from the WRF simulation were then converted into CMAQ meteorological field input using the Meteorology–Chemistry Interface Processor (MCIP) version 5.3.3.

2.3. Emission Inventories

Various emission inventories were used to produce emission data for the CMAQ model in this research. For OBB, emission data from the Fire Inventory from NCAR (FINN) version 1.5 [61] were used. Similarly to previous research [62], FINN was chosen for this study due to its finer spatial and temporal resolution (1 km, daily) for the year of interest. It is superior to other emission inventories, such as the Global Fire Emissions Database (GFED) [63], which provides monthly data at a 0.25-degree resolution, and the Global Fire Assimilation System (GFAS) [64], which provides daily data at a 0.1-degree resolution.

Moreover, FINN version 1.5 has been reported to yield the best performance for simulating $PM_{2.5}$ in the region of Southeast Asia, outperforming other inventories, as well as the newer FINN version 2.5 [65]. In order to avoid large fire emissions being confined solely to the surface layer, emissions from OBB were assumed to be uniformly distributed from the surface to the height of the planetary boundary layer (PBL). This assumption is supported by previous studies; moderately sized fires on a landscape scale, such as crop or grassland fires, seem to primarily emit their smoke into the PBL [66], and $PM_{2.5}$ concentrations simulated with CMAQ were not significantly affected by alterations in the injection height of fire emissions within the PBL and were not affected by emissions released into the free atmosphere [67,68].

After conducting a series of trial runs with the model, it was observed that the model overestimated $PM_{2.5}$ concentrations under conditions where the PBL height was relatively low. To address this issue, when the PBL height was less than 0.5 km, the emissions from OBB were assumed to be uniformly vertically distributed from the surface level to a height of 0.5 km instead of the actual PBL height. This adjustment was made through a process of trial and error. Many studies have also followed the same approach [69–74], highlighting the fact that setting up an atmospheric model for each scenario requires unique assumptions and modifications to accurately reflect the specific conditions being studied, as there is no universal method for setting up such models.

Emissions from other sources were derived from the following inventories: most of the anthropogenic emissions were from the Regional Emission Inventory in Asia (REAS) version 3.2 [75], which provides emission data only until 2015. Therefore, the 2015 data were used in this study to represent emissions in 2019. Marine and air traffic emissions were taken from the Task Force for Hemispheric Transport of Air Pollution (HTAP) version 2.2 [76], natural emissions were taken from the Model of Emissions of Gases and Aerosols from Nature (MEGAN) version 2.04 [77], and lastly, volcanic SO_2 emissions were taken from Carn et al. [78].

All emission inventories were combined using an in-house program to create two CMAQ-ready gridded emission inputs. The first gridded input contained solely OBB from FINN version 1.5, while the other included emissions from all other sources. Figure 2 visually illustrates the average emission intensities of both emission inputs.

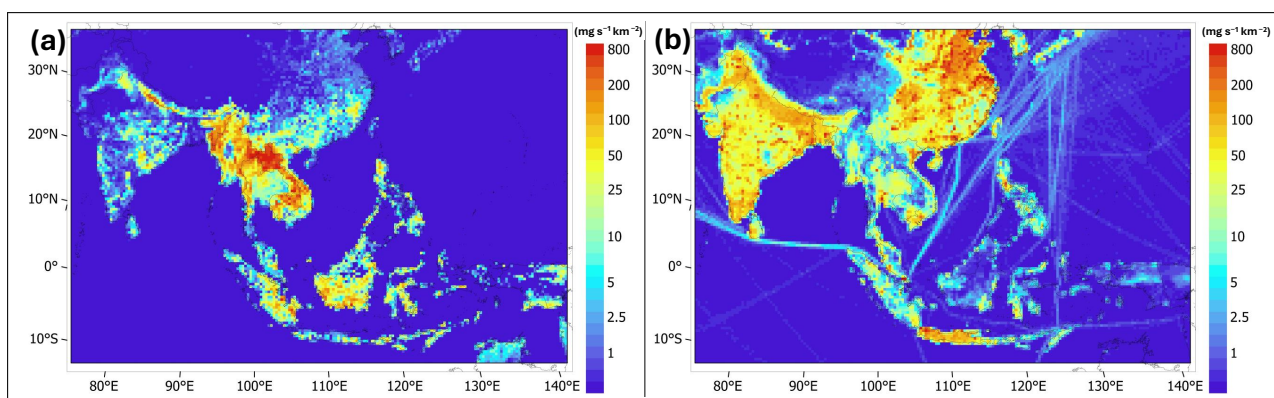


Figure 2. Average $PM_{2.5}$ emission intensities in the modeling domain: (a) emissions from open biomass burning and (b) emissions from other sources.

In the modeling domain, the total $PM_{2.5}$ emissions from OBB amounted to 8.81 Tg/year, while other emission sources contributed 18.79 Tg/year. Among the target source countries, Laos had the highest annual $PM_{2.5}$ emissions from OBB at 2.23 Tg/year. This was followed by Myanmar with 2.02 Tg/year, Thailand with 0.97 Tg/year, Vietnam with 0.84 Tg/year, and Cambodia with 0.68 Tg/year.

2.4. Source Apportionment

To perform nation-by-nation source apportionment, the built-in Integrated Source Apportionment Method (ISAM) tool [79,80] was used to individually track PM_{2.5} from OBB in each target source country. Region masks were applied, and five tags were assigned accordingly: Thailand (THA), Laos (LAO), Myanmar (MYA), Cambodia (CAM), and Vietnam (VNM). In addition, another tag (ETC) was assigned to track PM_{2.5} from OBB outside the nations of interest.

The overall contribution of OBB was calculated by dividing simulated PM_{2.5} values by the sum of values from the THA, LAO, MYA, CAM, VNM, and ETC tags, with the remaining percentage representing contributions from non-OBB sources. Similarly, the contributions from each target source country were calculated by dividing values from each tag by the simulated PM_{2.5} concentration.

2.5. Observation Data and Model Evaluation

The performance of the CMAQ model in reproducing the spatiotemporal variations in the PM_{2.5} concentration was evaluated by comparing simulated values with ground-level observed values from monitoring stations. Observed values from nine monitoring stations across seven Southeast Asian countries, which were provided by the Acid Deposition Monitoring Network in East Asia (EANET) [81], were used. In addition, the PM_{2.5} concentration in Thailand was further evaluated using observed data from 13 monitoring stations in the Upper Northern Region and 17 monitoring stations in the BMR, which were provided by the PCD through their official air quality report website (<http://air4thai.pcd.go.th/webV3/#/History>, accessed on 18 December 2023). The locations of all PCD and EANET stations used for model evaluation are shown in Figure 1.

Since the model output was in a gridded format, with each grid cell representing a mean PM_{2.5} concentration over the corresponding geographic area, the simulated value for each grid cell was compared with the observed value at the monitoring station located within that grid. If multiple monitoring stations were located within the same simulation grid, the average of the observed values from all stations in that grid was used for comparison. The statistical metrics used for the comparison included the Pearson correlation coefficient (*r*), Normalized Mean Bias (NMB), and Normalized Mean Error (NME). Detailed formulas for each metric are provided in Appendix A.

3. Results and Discussion

3.1. Model Performance

The monthly average observed PM_{2.5} concentrations from monitoring stations were compared with the simulation results for the BMR, WUN, CUN, and EUN regions, as shown in Figure 3. In the BMR, the observed monthly average PM_{2.5} concentrations ranged from 14.0 to 52.9 µg/m³, with an annual average of 25.2 µg/m³, which was nearly at the threshold of the national standard of 25 µg/m³. The highest concentrations were observed in January. In contrast, the sub-areas within the Upper Northern Region (WUN, CUN, and EUN) exhibited significantly higher PM_{2.5} levels, with monthly averages ranging from 6.1 to 90.1 µg/m³. The annual average for the Upper Northern Region as a whole was 31.0 µg/m³, exceeding the national standard. All sub-areas in the Upper Northern Region experienced their peak monthly average concentrations in March. WUN had the highest PM_{2.5} pollution, with an annual average concentration of 33.1 µg/m³ and a peak monthly concentration of 102.5 µg/m³. The CUN had an annual average of 30.3 µg/m³ and a peak concentration of 66.8 µg/m³ in March, while the EUN had an annual average of 29.6 µg/m³ and a peak concentration of 90.2 µg/m³ in the same month.

These observed PM_{2.5} values aligned with those in a previous study [20], which showed that transboundary transport significantly contributes to PM_{2.5} levels, particularly in regions closer to the borders. WUN, which borders Myanmar, and EUN, which borders Laos, exhibited some of the highest PM_{2.5} concentrations, supporting the notion that pollutants from neighboring countries are likely to impact the air quality in these areas. In

contrast, the BMR and the CUN region, which do not share borders with other countries and are more urbanized, showed comparatively lower PM_{2.5} levels. Urban areas, such as Chiang Mai and Lampang in CUN, tend to have lower contributions from OBB due to the reduced prevalence of such activities in densely populated regions. This urban characteristic, combined with the lack of cross-border pollution, helps explain the lower PM_{2.5} levels observed in these areas.

The comparison of the observed and simulated PM_{2.5} values in Figure 4 and the results of the statistical evaluation in Table 1 demonstrated strong agreement, with correlation coefficients of 0.68 and 0.73 for the EANET and PCD stations, respectively. This highlighted the model’s ability to capture the spatial and temporal distribution of PM_{2.5} across the modeling domain. The NMB values of 12% at EANET stations and –8% at PCD stations indicated slight overestimation and underestimation, respectively, suggesting variability in model accuracy due to factors such as local emissions and meteorological conditions. According to Huang et al. [82], NMB values within ±30% are generally considered acceptable, affirming the model’s reliability. Similarly, according to the same study, the NME values of 41% for EANET and 11% for PCD fell within acceptable ranges, further confirming the model’s accuracy.

Additionally, the model effectively captured seasonal variations, particularly during intense burning episodes in the dry season, as shown in Figure 3. The regional correlation coefficients of 0.78 for BMR, 0.97 for WUN, 0.86 for CUN, and 0.96 for EUN demonstrate robust model performances across these areas.

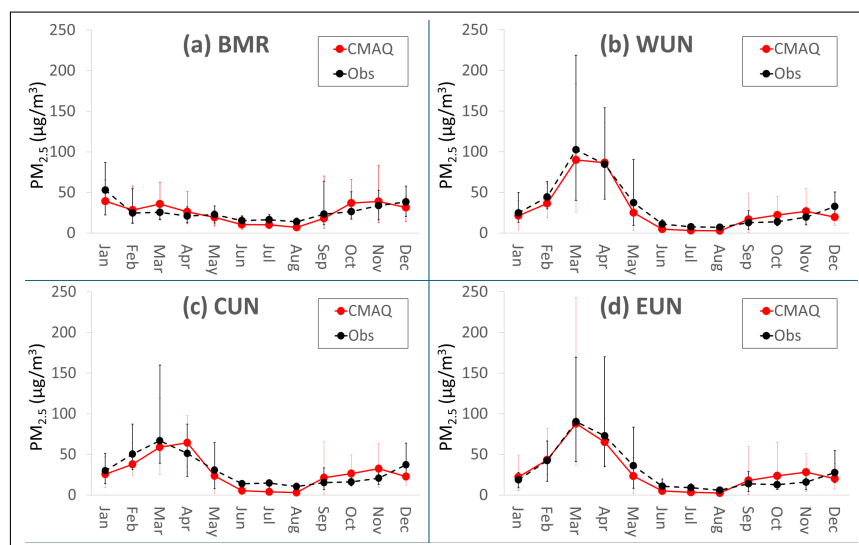


Figure 3. Time series of the observed (black line) and simulated (red line) monthly average PM_{2.5} concentrations in each target receptor area, with whiskers representing the range between minimum and maximum values: (a) BMR, (b) WUN, (c) CUN, and (d) EUN.

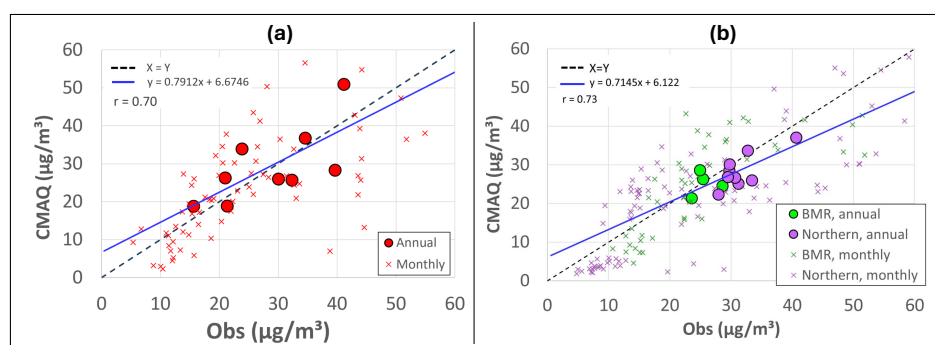


Figure 4. Comparison of the simulated and observed PM_{2.5} concentrations: (a) EANET stations and (b) PCD stations.

Table 1. Statistical metrics for the evaluation of the CMAQ model's performance. Monthly average values were used for calculation.

Monitoring Stations	Parameter (Unit)	Value
EANET	Mean CMAQ ($\mu\text{g}/\text{m}^3$)	31.11
	Mean obs ($\mu\text{g}/\text{m}^3$)	27.76
	r	0.68
	NMB (%)	12.0
	NME (%)	41.0
PCD (BMR+Upper Northern)	Mean CMAQ ($\mu\text{g}/\text{m}^3$)	29.7
	Mean obs ($\mu\text{g}/\text{m}^3$)	27.65
	r	0.73
	NMB (%)	−8
	NME (%)	11
PCD (BMR)	Mean CMAQ ($\mu\text{g}/\text{m}^3$)	25.18
	Mean obs ($\mu\text{g}/\text{m}^3$)	26.28
	r	0.78
	NMB (%)	−4
	NME (%)	26
PCD (WUN)	Mean CMAQ ($\mu\text{g}/\text{m}^3$)	29.53
	Mean obs ($\mu\text{g}/\text{m}^3$)	33.14
	r	0.97
	NMB (%)	−11
	NME (%)	22
PCD (CUN)	Mean CMAQ ($\mu\text{g}/\text{m}^3$)	27.04
	Mean obs ($\mu\text{g}/\text{m}^3$)	30.27
	r	0.86
	NMB (%)	−9
	NME (%)	32
PCD (EUN)	Mean CMAQ ($\mu\text{g}/\text{m}^3$)	28.47
	Mean obs ($\mu\text{g}/\text{m}^3$)	29.62
	r	0.96
	NMB (%)	−4
	NME (%)	21

3.2. Nation-by-Nation Contribution Assessment Results

Figure 5 shows the spatial distribution of the annual average and the March–April average $\text{PM}_{2.5}$ concentrations as simulated by the model. The figure clearly demonstrates that the $\text{PM}_{2.5}$ levels over Southeast Asia, particularly in Northern Thailand, Myanmar, and Laos, were significantly higher during March and April compared with the annual average. In Thailand, the model showed an annual average $\text{PM}_{2.5}$ concentration of $20.1 \mu\text{g}/\text{m}^3$, which increased sharply to $40.0 \mu\text{g}/\text{m}^3$ during March and April, nearly doubling. Comparing these results with the input OBB emission data in Figure 2 confirmed that OBB was the primary driver of this sharp increase in $\text{PM}_{2.5}$ levels. During the intense burning period, Laos experienced the highest $\text{PM}_{2.5}$ concentrations, followed by Myanmar and Thailand, which aligned with the previously described emission intensities. These findings highlight the substantial impact of OBB during intense burning episodes, highlighting how these activities significantly degrade air quality across the region during the dry season.

Figure 6 illustrates the spatial distribution of the annual contribution from OBB in each target source country, while Figure 7 shows the spatial distribution of the contributions during the intense burning period from March to April. Comparing these two figures revealed that the $\text{PM}_{2.5}$ levels from OBB in all target countries were significantly higher during the March–April period compared with the annual average. This comparison supports the conclusion that the sharp increase in $\text{PM}_{2.5}$ concentrations during this time was primarily driven by OBB, highlighting its crucial role in air quality degradation during the peak burning season.

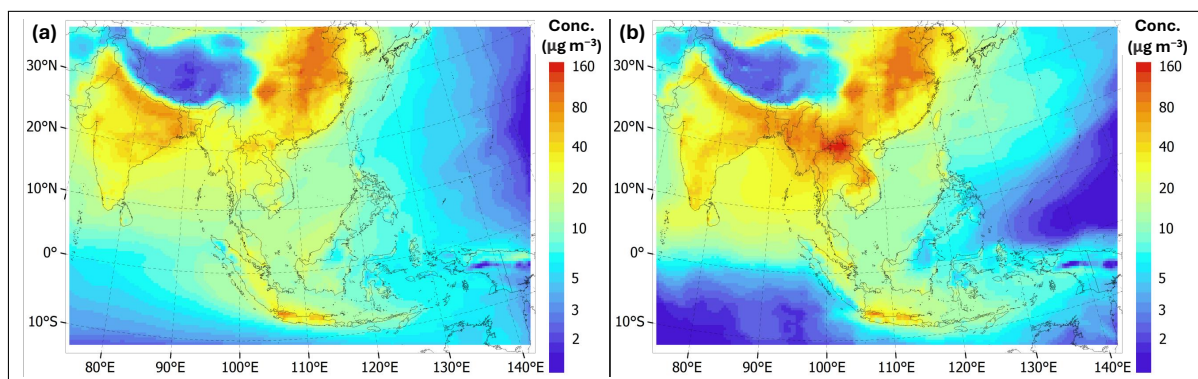


Figure 5. Spatial distribution of simulated PM_{2.5} concentrations: (a) annual average and (b) average during the intensive burning period (March–April).

Figures 8 and 9 summarize the annual contributions from OBB and the contributions from OBB during March and April, respectively, in each target source country. The contribution assessment results for the BMR indicated that OBB contributed only 15.3% to the annual average PM_{2.5} concentration. Compared with the Upper Northern Region, where OBB was a significant contributor, its impact on the BMR was relatively minor in comparison with other pollution sources. These results contradict those of a previous study [83–85], which reported that OBB was the primary or secondary contributor to PM_{2.5} in the BMR, with contributions ranging from 20% to 40%. The differences in these findings were likely due to differences in methodology. While those studies utilized receptor modeling, which estimates source contributions at specific sites based on the chemical analysis of air samples, this study employs an atmospheric chemical transport model. The transport model enables a more comprehensive analysis across a larger spatial domain, capturing both local and transboundary pollution. Furthermore, the previous studies were limited to 2–4 specific urban and suburban sites, which may not fully account for regional or transboundary contributions.

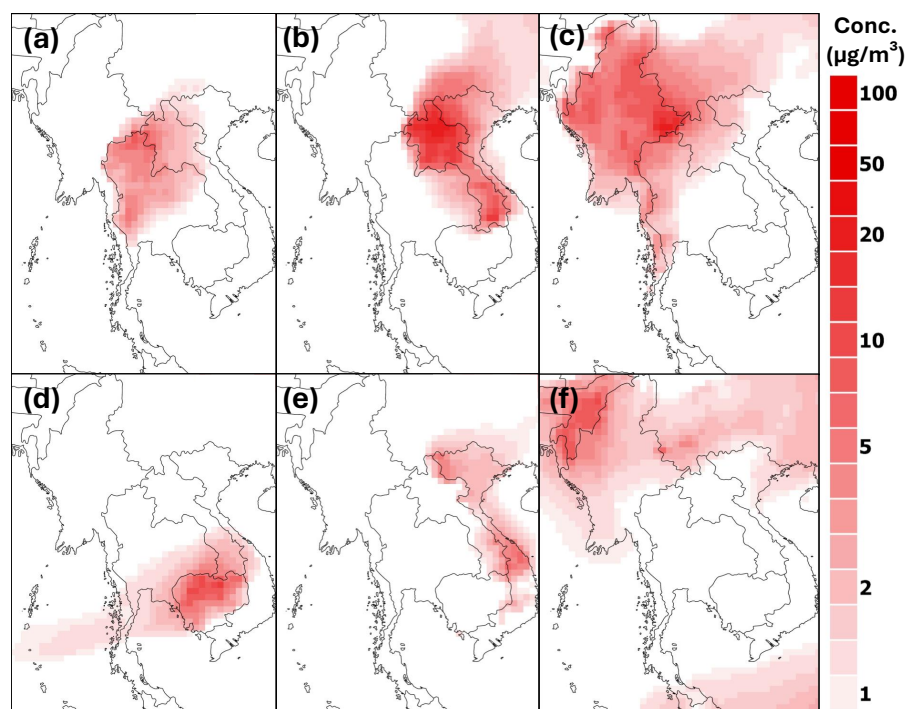


Figure 6. Average annual contribution of PM_{2.5} concentrations due to OBB in each target source country: (a) Thailand, (b) Laos, (c) Myanmar, (d) Cambodia, (e) Vietnam, and (f) other countries.

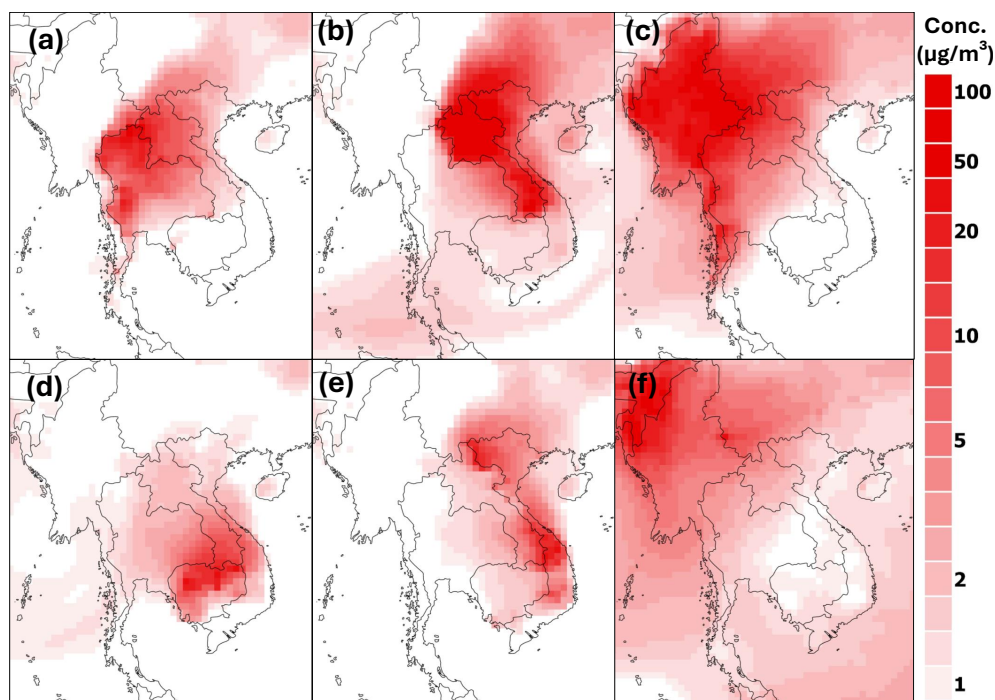


Figure 7. Spatial distribution of PM_{2.5} from OBB in each target source country during March–April: (a) Thailand, (b) Laos, (c) Myanmar, (d) Cambodia, (e) Vietnam, and (f) other countries.

Despite the relatively minor overall impact of OBB on the PM_{2.5} levels in the BMR, the influence of transboundary transport remained significant, even when considering the distance from international borders. Notably, domestic OBB accounted for only 2.5% of the annual PM_{2.5} in the BMR, while transboundary transport contributed 12.7%, with Myanmar being the largest contributor at 3.5%. During the intense burning period from March to April, the contribution from OBB to PM_{2.5} in the BMR increased significantly to 31.7%, of which only 4.7% was from local sources, while the remaining 27% was due to transboundary transport, with Myanmar again being the most significant contributor (12.3%). This highlighted that, although less pronounced than in the Upper Northern Region, transboundary transport still significantly impacted the PM_{2.5} levels in the BMR during peak burning periods.

For the Upper Northern Region, the contribution assessment results indicated that OBB significantly impacted PM_{2.5} levels, contributing 43.0%, 29.9%, and 41.8% to the annual PM_{2.5} concentrations in the WUN, CUN, and EUN sub-areas, respectively. During the intensive burning period in March and April, these contributions increased to 61.9%, 48.1%, and 60.2%, respectively. Myanmar was the most significant contributor to PM_{2.5} levels in WUN, with contributions of 19.7% annually and 31.5% during the intense burning period. For CUN, while Thailand was the largest contributor annually at 12.7%, Myanmar became the most significant contributor during the peak months at 20.1%. In contrast, Thailand was the major contributor to EUN both annually and during the peak months, with contributions of 18.6% and 25.6%, respectively.

The results also revealed that transboundary transport had a greater influence on PM_{2.5} levels in the Upper Northern Region than domestic burning, contributing 29.5%, 17.1%, and 23.1% annually in the WUN, CUN, and EUN sub-regions, respectively. During the peak burning months, these contributions increased to 42.4%, 28.6%, and 34.6% in WUN, CUN, and EUN, respectively. These findings were consistent with those of previous research [20], which reported similar percentages of contributions from transboundary transport in the provinces within the WUN and EUN sub-regions. However, for CUN, the contribution percentages reported in this study were slightly lower, which was likely due to differences in the modeling framework and emission inventories used. WUN and EUN were more affected by transboundary transport due to their proximity to international

borders, whereas CUN, being more centrally located, was primarily influenced by domestic sources. Despite EUN’s proximity to Laos, the transboundary contribution from Laos (10.5%) was secondary to that of domestic burning (18.6%). Although Laos had the highest PM_{2.5} emissions from OBB, prevailing meteorological conditions caused the PM_{2.5} to be dispersed eastward, away from the Upper Northern Region of Thailand.

Despite the valuable insights from this study, several limitations should be acknowledged. First, the coarse spatial resolution of the model may reduce the accuracy of reproducing the spatiotemporal variations in PM_{2.5}, particularly in areas with complex terrain. A finer resolution could provide a clearer view of pollution dispersion patterns. Second, the lack of an up-to-date emission inventory for the study year required the use of older data as a proxy, so year-specific variations may not have been captured. These limitations emphasize the need for future research with improved spatial resolution and updated emission data to better understand the contributions from OBB and other sources.

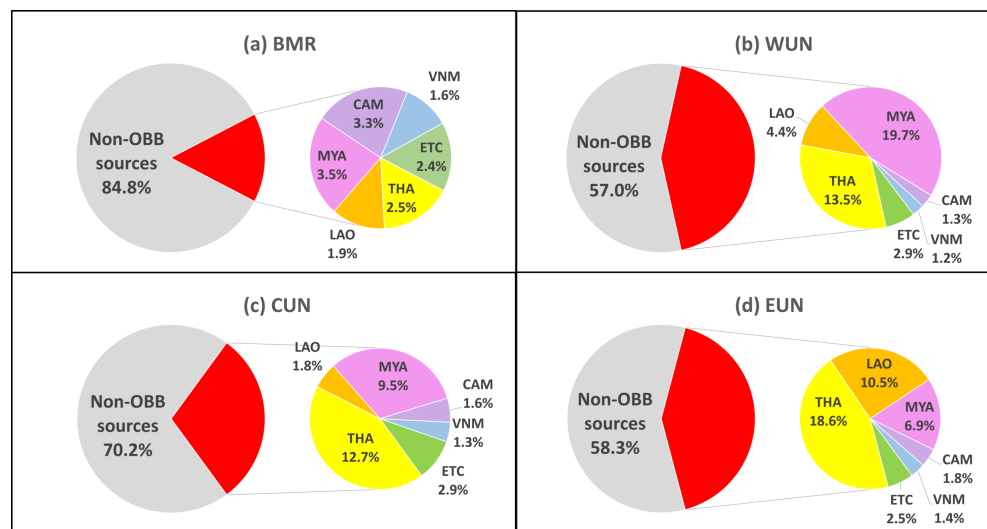


Figure 8. Annual nation-by-nation contributions from OBB to the PM_{2.5} concentrations in each target receptor area: (a) BMR, (b) WUN, (c) CUN, and (d) EUN.

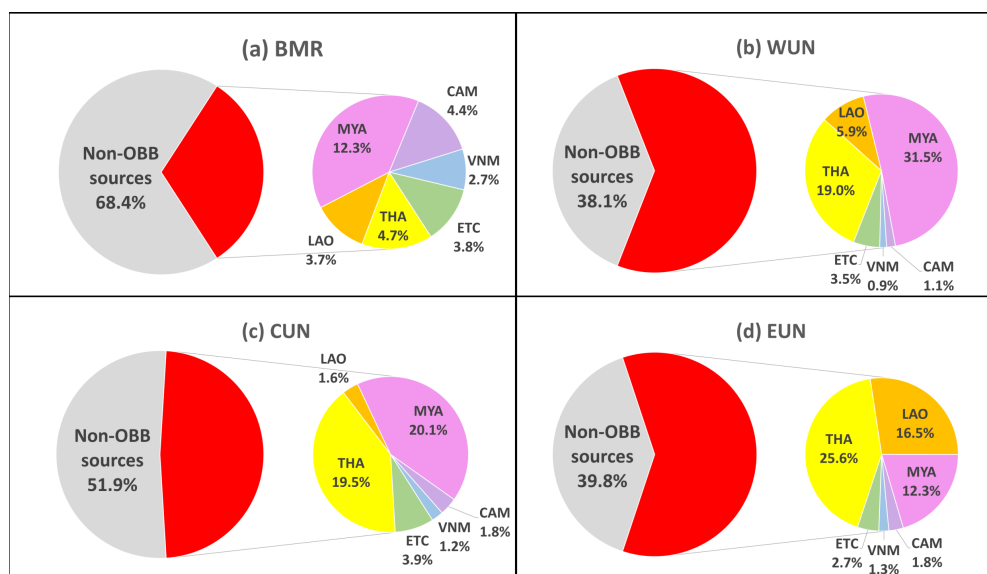


Figure 9. Nation-by-nation contributions from OBB to PM_{2.5} concentrations from March to April in each target receptor area: (a) BMR, (b) WUN, (c) CUN, and (d) EUN.

4. Conclusions

This study employed the Community Multiscale Air Quality (CMAQ) atmospheric chemical transport model to assess the contributions of open biomass burning (OBB) from target source countries to PM_{2.5} concentrations in the Upper Northern Region of Thailand and the Bangkok Metropolitan Region (BMR). The Upper Northern Region was further divided into three sub-regions based on geographical borders: West, Central, and East Upper Northern (WUN, CUN, and EUN). The target source countries considered were Thailand, Myanmar, Laos, Cambodia, and Vietnam. The CMAQ model was used to simulate the spatiotemporal variations in PM_{2.5} concentrations throughout 2019 over a wide Asian domain. Model performance was then evaluated by comparing the simulation results with observed data from the Acid Deposition Monitoring Network in East Asia (EANET) and the Thai Pollution Control Department (PCD). The model demonstrated a strong ability to replicate the spatiotemporal variations in PM_{2.5} across the study domain, with correlation coefficients of 0.68 and 0.73 for the EANET and PCD stations, respectively. The Integrated Source Apportionment Method (ISAM) tool was then applied to quantify the contributions of local OBB and transboundary transport from the target source countries.

The results from contribution analysis indicated that the overall impact of OBB on the BMR was relatively minor compared with that of other pollution sources, which was likely due to its urban setting. OBB contributed only 15.3% to the annual PM_{2.5} concentration with Myanmar as the primary contributor. However, during the peak burning period from March to April, the contribution increased to 31.7%, with the transboundary transport from Myanmar remaining as the most significant contributor, accounting for 12.7%.

In contrast, OBB significantly impacted the PM_{2.5} levels in the Upper Northern Region, contributing 43.0%, 29.9%, and 41.8% to the annual PM_{2.5} concentrations in the WUN, CUN, and EUN sub-regions, respectively. These contributions increased substantially during the peak burning period in March and April, reaching 61.9% in WUN, 48.1% in CUN, and 60.2% in EUN. Among the contributors, Myanmar was the most significant source of PM_{2.5} in WUN, contributing 19.7% annually and 31.5% during peak months. In CUN, Thailand was the main annual contributor (12.7%), while Myanmar dominated during peak burning (20.1%). In EUN, despite proximity to Laos, where OBB emissions are the highest in the region, Thailand contributed the most, with 18.6% annually and 25.6% during peak burning. The prevailing meteorological conditions caused PM_{2.5} from OBB in Laos to be dispersed eastward, away from Thailand.

Overall, these findings highlighted that transboundary transport had a more significant impact on the PM_{2.5} levels in Thailand than that of domestic burning and that regional cooperation and comprehensive strategies are needed to effectively mitigate pollution. This study's limitations include the use of a coarse spatial resolution, which may have affected the accuracy of PM_{2.5} simulations in complex terrains, and the reliance on older emission inventory data. Future research employing higher spatial resolution and updated emission inventories is essential for refining the understanding of contributions from OBB and other sources.

Author Contributions: Conceptualization, N.C. and H.S.; methodology, N.C. and H.S.; software, N.C. and H.S.; validation, N.C. and H.S.; formal analysis, N.C.; resources, H.S. and A.K.; data curation, N.C., H.S. and K.U.; writing—original draft preparation, N.C.; writing—review and editing, N.C., H.S., K.U., L.V.M., T.M. and A.K.; visualization, N.C.; supervision, H.S.; project administration, H.S.; funding acquisition, H.S. All authors have read and agreed to the published version of the manuscript.

Funding: This research was funded by the Environment Research and Technology Development Fund (Grant Number JPMEERF20215005) of the Environmental Restoration and Conservation Agency provided by the Ministry of Environment of Japan and JSPS KAKENHI (Grant Number 23K25011).

Institutional Review Board Statement: Not applicable

Informed Consent Statement: Not applicable

Data Availability Statement: The original contributions presented in the study are included in the article, further inquiries can be directed to the corresponding author.

Conflicts of Interest: The authors declare no conflicts of interest. The funders had no role in the design of the study; in the collection, analyses, or interpretation of data; in the writing of the manuscript; or in the decision to publish the results.

Abbreviations

The following abbreviations are used in this manuscript:

BMR	Bangkok Metropolitan Region
CMAQ	Community Multiscale Air Quality
CUN	Central Upper Northern
EANET	Acid Deposition Monitoring Network in East Asia
ERA5	ECMWF Reanalysis version 5
EUN	East Upper Northern
FINN	Fire Inventory from NCAR
GFAS	Global Fire Assimilation System
GFED	Global Fire Emissions Database
GMTED	Global Multi-Resolution Terrain Elevation Data
HTAP	Task Force for Hemispheric Transport of Air Pollution
ISAM	Integrated Source Apportionment Method
MCIP	Meteorology–Chemistry Interface Processor
MEGAN	Model of Emissions of Gases and Aerosols from Nature
MODIS	Moderate Resolution Imaging Spectroradiometer
NMB	Normalized Mean Bias
NME	Normalized Mean Error
OBB	Open Biomass Burning
PBL	Planetary Boundary Layer
PCD	Pollution Control Department
PM _{2.5}	Particulate matter with a diameter smaller than 2.5 μm
PMF	Positive Matrix Factorization
PSCF	Potential Source Contribution Function
REAS	Regional Emission Inventory in Asia
SAPRC	State Air Pollution Research Center
WACCM	Whole Atmosphere Community Climate Model
WRF	Weather Research and Forecasting
WUN	West Upper Northern

Appendix A. Formulas for Model Evaluation Metrics

Pearson correlation coefficient (r):

$$r = \frac{\sum_{i=1}^n (O_i - \bar{O})(S_i - \bar{S})}{\sqrt{\sum_{i=1}^n (O_i - \bar{O})^2 \sum_{i=1}^n (S_i - \bar{S})^2}} \quad (\text{A1})$$

Normalized Mean Bias (NMB):

$$\text{NMB} = \frac{\sum_{i=1}^n (S_i - O_i)}{\sum_{i=1}^n O_i} \times 100\% \quad (\text{A2})$$

Normalized Mean Error (NME):

$$\text{NME} = \frac{\sum_{i=1}^n |S_i - O_i|}{\sum_{i=1}^n O_i} \times 100\% \quad (\text{A3})$$

where the following are denoted:

- O_i is the observed value for observation i ;
- S_i is the simulated value for observation i ;

- \bar{O} is the mean of observed values;
- \bar{S} is the mean of simulated values;
- n is the total number of observations.
- NMB and NME are expressed as a percentage by multiplying the result by 100%.

References

- Vadrevu, K.; Lasko, K.; Giglio, L.; Schroeder, W.; Biswas, S.; Justice, C. Trends in Vegetation fires in South and Southeast Asian Countries. *Sci. Rep.* **2019**, *9*, 7422. [[CrossRef](#)] [[PubMed](#)]
- Inoue, Y.; Kiyono, Y.; Asai, H.; Ochiai, Y.; Qi, J.; Olioso, A.; Tatsuhiko, S.; Horie, T.; Saito, K.; Dounagsavanh, L. Assessing land-use and carbon stock in slash-and-burn ecosystems in tropical mountain of Laos based on time-series satellite images. *Int. J. Appl. Earth Obs. Geoinf.* **2010**, *12*, 287–297. [[CrossRef](#)]
- Yin, S. Biomass burning spatiotemporal variations over South and Southeast Asia. *Environ. Int.* **2020**, *145*, 106153. [[CrossRef](#)] [[PubMed](#)]
- Oanh, N.T.; Ly, B.T.; Tipayarom, D.; Manadhar, B.; Pongkiatkul, P.; Simpson, C.; Liu, L.J. Characterization of particulate matter emission from open burning of rice straw. *Atmos. Environ.* **2011**, *45*, 493–502. [[CrossRef](#)] [[PubMed](#)]
- Hays, M.D.; Fine, P.M.; Geron, C.D.; Kleeman, M.J.; Gullett, B.K. Open burning of agricultural biomass: Physical and chemical properties of particle-phase emissions. *Atmos. Environ.* **2005**, *39*, 6747–6764. [[CrossRef](#)]
- Nyamadzawo, G.; Wuta, M.; Nyamangara, J.; Nyamugafata, P.; Tendayi, T. Burning, biomass removal and tillage effects on soil organic carbon and nutrients in seasonal wetlands (Dambos) of Chiota smallholder farming area, Zimbabwe. *Archives of Agronomy and Soil. Arch. Agron. Soil Sci.* **2014**, *60*, 1411–1427. [[CrossRef](#)]
- Brye, K.R. Long-term Effects of Aboveground Biomass Removal by Burning on Potential Nutrient Recycling. *Crop Manag.* **2012**, *11*, 1–9. [[CrossRef](#)]
- Lee, H.H.; Iraqui, O.; Gu, Y.; Yim, S.H.L.; Chulakadabba, A.; Tonks, A.Y.M.; Yang, Z.; Wang, C. Impacts of air pollutants from fire and non-fire emissions on the regional air quality in Southeast Asia. *Atmos. Chem. Phys.* **2018**, *18*, 6141–6156. [[CrossRef](#)]
- Chen, J.; Li, C.; Ristovski, Z.; Milic, A.; Gu, Y.; Islam, M.S.; Wang, S.; Hao, J.; Zhang, H.; He, C.; et al. A review of biomass burning: Emissions and impacts on air quality, health and climate in China. *Sci. Total Environ.* **2017**, *579*, 1000–1034. [[CrossRef](#)]
- Vajanapoom, N.; Kooncumchoo, P.; Thach, T.Q. Acute effects of air pollution on all-cause mortality: A natural experiment from haze control measures in Chiang Mai Province, Thailand. *PeerJ* **2020**, *8*, e9207. [[CrossRef](#)]
- Pavagadhi, S.; Betha, R.; Venkatesan, S.; Balasubramanian, R.; Hande, M.P. Physicochemical and toxicological characteristics of urban aerosols during a recent Indonesian biomass burning episode. *Environ. Sci. Pollut. Res.* **2013**, *20*, 2569–2578. [[CrossRef](#)] [[PubMed](#)]
- Chomane, J.; Thongboon, K.; Tekasakul, S.; Furuuchi, M.; Dejchanchaiwong, R.; Tekasakul, P. Physicochemical and toxicological characteristics of nanoparticles in aerosols in southern Thailand during recent haze episodes in lower southeast Asia. *J. Environ. Sci.* **2020**, *94*, 72–80. [[CrossRef](#)] [[PubMed](#)]
- Yin, S.; Wang, X.; Zhang, X.; Guo, M.; Miura, M.; Xiao, Y. Influence of biomass burning on local air pollution in mainland Southeast Asia from 2001 to 2016. *Environ. Pollut.* **2019**, *254*, 112949. [[CrossRef](#)] [[PubMed](#)]
- Weichenthal, S.; Kulka, R.; Lavigne, E.; Rijswijk, D.; Brauer, M.; Villeneuve, P.; Stieb, D.; Joseph, L.; Burnett, R. Biomass Burning as a Source of Ambient Fine Particulate Air Pollution and Acute Myocardial Infarction. *Epidemiology* **2017**, *28*, 329–337. [[CrossRef](#)]
- Linh Thao, N.N.; Pimonsree, S.; Prueksakorn, K.; Bich Thao, P.T.; Vongruang, P. Public health and economic impact assessment of PM2.5 from open biomass burning over countries in mainland Southeast Asia during the smog episode. *Atmos. Pollut. Res.* **2022**, *13*, 101418. [[CrossRef](#)]
- Fongsodsri, K.; Chamnanchanunt, S.; Desakorn, V.; Thanachartwet, V.; Sahassananda, D.; Rojnuckarin, P.; Umemura, T. Particulate Matter 2.5 and Hematological Disorders From Dust to Diseases: A Systematic Review of Available Evidence. *Front. Med.* **2021**, *8*, 692008. [[CrossRef](#)]
- Xing, Y.F.; Xu, Y.H.; Shi, M.H.; Lian, Y.X. The impact of PM2.5 on the human respiratory system. *J. Thorac. Dis.* **2016**, *8*, E69–E74. [[CrossRef](#)]
- Krittanawong, C.; Qadeer, Y.K.; Hayes, R.B.; Wang, Z.; Thurston, G.D.; Virani, S.; Lavie, C.J. PM2.5 and cardiovascular diseases: State-of-the-Art review. *Int. J. Cardiol. Cardiovasc. Risk Prev.* **2023**, *19*, 200217. [[CrossRef](#)]
- Targino, A.C.; Krecl, P.; Johansson, C.; Swietlicki, E.; Massling, A.; Coraiola, G.C.; Lihavainen, H. Deterioration of air quality across Sweden due to transboundary agricultural burning emissions. *Boreal Environ. Res.* **2013**, *18*, 19.
- Inlaung, K.; Chotamonsak, C.; Macatangay, R.; Surapipith, V. Assessment of Transboundary PM2.5 from Biomass Burning in Northern Thailand Using the WRF-Chem Model. *Toxics* **2024**, *12*, 462. [[CrossRef](#)]
- Yang, L.; Gao, X.; Li, Z.; Jia, D. Quantitative effects of air pollution on regional daily global and diffuse solar radiation under clear sky conditions. *Energy Rep.* **2022**, *8*, 1935–1948. [[CrossRef](#)]
- Yang, L.; Gao, X.; Li, Z.; Jia, D. Intra-day solar irradiation forecast using machine learning with satellite data. *Sustain. Energy Grids Netw.* **2023**, *36*, 101212. [[CrossRef](#)]
- Cai, Z.Y.; Yao, Q.; Han, S.Q.; Liu, J.L. The influence of the air quality and meteorological field about Aerosol direct climate effect on Tianjin. *Zhongguo Huanjing Kexue/China Environ. Sci.* **2017**, *37*, 908–914.

24. Huang, Y.; Shen, H.; Chen, H.; Wang, R.; Zhang, Y.; Su, S.; Chen, Y.; Lin, N.; Zhuo, S.; Zhong, Q.; et al. Quantification of Global Primary Emissions of PM_{2.5}, PM₁₀, and TSP from Combustion and Industrial Process Sources. *Environ. Sci. Technol.* **2014**, *48*, 13834–13843. [[CrossRef](#)] [[PubMed](#)]
25. Li, Y.; Zhou, L.; Liu, H.; Liu, S.; Feng, M.; Song, D.; Tan, Q.; Jiang, H.; Zuoqiu, S.; Yang, F. Disparities in precipitation effects on PM_{2.5} mass concentrations and chemical compositions: Insights from online monitoring data in Chengdu. *J. Environ. Sci.* **2024**, *in press*. [[CrossRef](#)]
26. Pollution Control Department. *Thailand State of Pollution Report 2022*; Technical Report; Pollution Control Department, Ministry of Resources and Environment: Bangkok, Thailand, 2023.
27. Amnuaylojaroen, T.; Inkom, J.; Janta, R.; Surapipith, V. Long Range Transport of Southeast Asian PM_{2.5} Pollution to Northern Thailand during High Biomass Burning Episodes. *Sustainability* **2020**, *12*, 10049. [[CrossRef](#)]
28. Suriyawong, P.; Chuetor, S.; Samae, H.; Piriyaakarnsakul, S.; Amin, M.; Furuuchi, M.; Hata, M.; Inerb, M.; Phairuang, W. Airborne particulate matter from biomass burning in Thailand: Recent issues, challenges, and options. *Heliyon* **2023**, *9*, e14261. [[CrossRef](#)]
29. Chantarapachoom, N.; Mochizuki, D.; Shimadera, H.; Luong, M.; Matsuo, T.; Kondo, A. Impact assessment of biomass burning in Southeast Asia to 2019 annual average PM_{2.5} concentration in Thailand using atmospheric chemical transport model. *E3S Web Conf.* **2023**, *379*, 01002. [[CrossRef](#)]
30. Punsompong, P.; Pani, S.K.; Wang, S.H.; Bich Pham, T.T. Assessment of biomass-burning types and transport over Thailand and the associated health risks. *Atmos. Environ.* **2021**, *247*, 118176. [[CrossRef](#)]
31. World Health Organization. *WHO Global Air Quality Guidelines: Particulate Matter (PM_{2.5} and PM₁₀), Ozone, Nitrogen Dioxide, Sulfur Dioxide and Carbon Monoxide*; World Health Organization: Geneva, Switzerland, 2021; p. xxi, 273.
32. Kasiravat, P.; Ingviya, T. Effects of fine particulate matter on hospital admission due to stroke in a business city of Thailand. *Chulalongkorn Med. J.* **2023**, *67*. [[CrossRef](#)]
33. Jaremwong, K.; Gheewala, S.H.; Sampattagul, S. Health Impact Related to Ambient Particulate Matter Exposure as a Spatial Health Risk Map Case Study in Chiang Mai, Thailand. *Atmosphere* **2023**, *14*, 261. [[CrossRef](#)]
34. Nakhartai, N.; Traisathit, P.; Thongsak, N.; Supasri, T.; Srikummoon, P.; Thumronglaohapun, S.; Hemwan, P.; Chitapanarux, I. Impact of Residential Concentration of PM_{2.5} Analyzed as Time-Varying Covariate on the Survival Rate of Lung Cancer Patients: A 15-Year Hospital-Based Study in Upper Northern Thailand. *Int. J. Environ. Res. Public Health* **2022**, *19*, 4521. [[CrossRef](#)] [[PubMed](#)]
35. Supasri, T.; Gheewala, S.; Macatangay, R.; Chakpor, A.; Sedpho, S. Association between ambient air particulate matter and human health impacts in northern Thailand. *Sci. Rep.* **2023**, *13*, 12753. [[CrossRef](#)] [[PubMed](#)]
36. Pornchanok Praditthong, N.H.; Maneejuk, P. The Impact Of Particulate Matter 2.5 On Tourist Arrival In Chiang Mai. *J. Posit. Sch. Psychol.* **2022**, *6*, 3151–3160.
37. Namcome, T.; Tansuchat, R. The Impact of Fine Particulate Matter (PM 2.5) Pollution on the Number of Foreign Tourists in Chiang Mai and Bangkok. *Community Soc. Dev. J. (In Thai)* **2021**, *22*, 19–35. Available online: <https://so05.tci-thaijo.org/index.php/cmruresearch/article/view/247437>(accessed on 3 October 2024).
38. Srinamphon, P.; Chernbumroong, S.; Tippayawong, K.Y. The Effect of Small Particulate Matter on Tourism and Related SMEs in Chiang Mai, Thailand. *Sustainability* **2022**, *14*, 8147. [[CrossRef](#)]
39. Hassan Bran, S.; Macatangay, R.; Chotamonsak, C.; Chantara, S.; Surapipith, V. Understanding the seasonal dynamics of surface PM_{2.5} mass distribution and source contributions over Thailand. *Atmos. Environ.* **2024**, *331*, 120613. [[CrossRef](#)]
40. Song, W.; Zhang, Y.L.; Zhang, Y.; Cao, F.; Rauber, M.; Salazar, G.; Kawichai, S.; Prapamontol, T.; Szidat, S. Is biomass burning always a dominant contributor of fine aerosols in upper northern Thailand? *Environ. Int.* **2022**, *168*, 107466. [[CrossRef](#)]
41. Chansuebsri, S.; Kolar, P.; Kraitsitnikul, P.; Kantarawilawan, N.; Yabueng, N.; Wiriya, W.; Thepnuan, D.; Chantara, S. Chemical composition and origins of PM_{2.5} in Chiang Mai (Thailand) by integrated source apportionment and potential source areas. *Atmos. Environ.* **2024**, *327*, 120517. [[CrossRef](#)]
42. Pollution Control Department. *Thailand State of Pollution Report 2019*; Technical Report; Pollution Control Department, Ministry of Resources and Environment: Bangkok, Thailand, 2020.
43. Pani, S.K.; Chantara, S.; Khamkaew, C.; Lee, C.T.; Lin, N.H. Biomass burning in the northern peninsular Southeast Asia: Aerosol chemical profile and potential exposure. *Atmos. Res.* **2019**, *224*, 180–195. [[CrossRef](#)]
44. Jainontee, K.; Pongkiatkul, P.; Wang, Y.L.; Weng, R.J.; Lu, Y.T.; Wang, T.S.; Chen, W.K. Strategy Design of PM_{2.5} Controlling for Northern Thailand. *Aerosol Air Qual. Res.* **2023**, *23*, 220432. [[CrossRef](#)]
45. National Statistical Office. *Number of Population from Registration by Sex, House, Region and Province: 2019–2022*; National Statistical Office: Bangkok, Thailand.
46. US EPA Office of Research and Development. *CMAQ*, version 5.3.3; Zenodo: Genève Switzerland, 2021. [[CrossRef](#)]
47. Saha, L.; Kumar, A.; Kumar, S.; Korstad, J.; Srivastava, S.; Baudhdh, K. The impact of the COVID-19 lockdown on global air quality: A review. *Environ. Sustain.* **2022**, *5*, 5–23. [[CrossRef](#)] [[PubMed](#)]
48. Addas, A.; Maghrabi, A. The Impact of COVID-19 Lockdowns on Air Quality—A Global Review. *Sustainability* **2021**, *13*, 10212. [[CrossRef](#)]
49. Carter, W.P. Development of the SAPRC-07 chemical mechanism. *Atmos. Environ.* **2010**, *44*, 5324–5335. [[CrossRef](#)]

50. Atmospheric Chemistry Observations and Modeling; National Center for Atmospheric Research; University Corporation for Atmospheric Research. *Whole Atmosphere Community Climate Model (WACCM) Model Output* (updated daily); Atmospheric Research, Computational and Information Systems Laboratory: Boulder, CO, USA, 2020; Research Data Archive at the National Center for Atmospheric Research. [[CrossRef](#)]
51. Skamarock, W.C.; Klemp, J.B.; Dudhia, J.; Gill, D.O.; Liu, Z.; Berner, J.; Wang, W.; Powers, J.G.; Duda, M.G.; Barker, D.; et al. *A Description of the Advanced Research WRF Model Version 4.3*; Technical Report; National Center for Atmospheric Research; University Corporation for Atmospheric Research: Boulder, CO, USA, 2021. [[CrossRef](#)]
52. Morrison, H.; Milbrandt, J.A. Parameterization of Cloud Microphysics Based on the Prediction of Bulk Ice Particle Properties. Part I: Scheme Description and Idealized Tests. *J. Atmos. Sci.* **2015**, *72*, 287–311. [[CrossRef](#)]
53. Iacono, M.J.; Delamere, J.S.; Mlawer, E.J.; Shephard, M.W.; Clough, S.A.; Collins, W.D. Radiative forcing by long-lived greenhouse gases: Calculations with the AER radiative transfer models. *J. Geophys. Res. Atmos.* **2008**, *113*, D13103–1–D13103–8. [[CrossRef](#)]
54. Olson, J.B.; Smirnova, T.; Kenyon, J.S.; Turner, D.D.; Brown, J.M.; Zheng, W.; Green, B.W. *A Description of the MYNN Surface-Layer Scheme*; Technical Report; National Oceanic and Atmospheric Administration, Oceanic and Atmospheric Research, Global Systems Laboratory: Boulder, CO, USA, 2021. [[CrossRef](#)]
55. Chen, F.; Dudhia, J. Coupling an Advanced Land Surface–Hydrology Model with the Penn State–NCAR MM5 Modeling System. Part I: Model Implementation and Sensitivity. *Mon. Weather Rev.* **2001**, *129*, 569–585. [[CrossRef](#)]
56. NAKANISHI, M.; NIINO, H. Development of an Improved Turbulence Closure Model for the Atmospheric Boundary Layer. *J. Meteorol. Soc. Japan. Ser. II* **2009**, *87*, 895–912. [[CrossRef](#)]
57. Grell, G.A.; Dévényi, D. A generalized approach to parameterizing convection combining ensemble and data assimilation techniques. *Geophys. Res. Lett.* **2002**, *29*, 38–1–38–4. [[CrossRef](#)]
58. Danielson, J.J.; Gesch, D.B. *Global Multi-Resolution Terrain Elevation Data 2010 (GMTED2010)*; Technical Report; Earth Resources Observation and Science (EROS) Center: Sioux Falls, SD, USA, 2011. [[CrossRef](#)]
59. Broxton, P.D.; Zeng, X.; Sulla-Menashe, D.; Troch, P.A. A Global Land Cover Climatology Using MODIS Data. *J. Appl. Meteorol. Climatol.* **2014**, *53*, 1593–1605. [[CrossRef](#)]
60. Hersbach, H.; Bell, B.; Berrisford, P.; Hirahara, S.; Horányi, A.; Muñoz-Sabater, J.; Nicolas, J.; Peubey, C.; Radu, R.; Schepers, D.; et al. The ERA5 global reanalysis. *Q. J. R. Meteorol. Soc.* **2020**, *146*, 1999–2049. [[CrossRef](#)]
61. Wiedinmyer, C.; Akagi, S.K.; Yokelson, R.J.; Emmons, L.K.; Al-Saadi, J.A.; Orlando, J.J.; Soja, A.J. The Fire INventory from NCAR (FINN): A high resolution global model to estimate the emissions from open burning. *Geosci. Model Dev.* **2011**, *4*, 625–641. [[CrossRef](#)]
62. Uranishi, K.; Ikemori, F.; Shimadera, H.; Kondo, A.; Sugata, S. Impact of field biomass burning on local pollution and long-range transport of PM_{2.5} in Northeast Asia. *Environ. Pollut.* **2019**, *244*, 414–422. [[CrossRef](#)] [[PubMed](#)]
63. Giglio, L.; Randerson, J.T.; van der Werf, G.R. Analysis of daily, monthly, and annual burned area using the fourth-generation global fire emissions database (GFED4). *J. Geophys. Res. Biogeosciences* **2013**, *118*, 317–328. [[CrossRef](#)]
64. Kaiser, J.W.; Heil, A.; Andreae, M.O.; Benedetti, A.; Chubarova, N.; Jones, L.; Morcrette, J.J.; Razinger, M.; Schultz, M.G.; Suttie, M.; et al. Biomass burning emissions estimated with a global fire assimilation system based on observed fire radiative power. *Biogeosciences* **2012**, *9*, 527–554. [[CrossRef](#)]
65. Thongsame, W.; Henze, D.K.; Kumar, R.; Barth, M.; Pfister, G. Evaluation of WRF-Chem PM_{2.5} simulations in Thailand with different anthropogenic and biomass-burning emissions. *Atmos. Environ. X* **2024**, *23*, 100282. [[CrossRef](#)]
66. Paugam, R.; Wooster, M.; Freitas, S.; Val Martin, M. A review of approaches to estimate wildfire plume injection height within large-scale atmospheric chemical transport models. *Atmos. Chem. Phys.* **2016**, *16*, 907–925. [[CrossRef](#)]
67. Garcia-Menendez, F.; Hu, Y.; Odman, M.T. Simulating smoke transport from wildland fires with a regional-scale air quality model: Sensitivity to spatiotemporal allocation of fire emissions. *Sci. Total Environ.* **2014**, *493*, 544–553. [[CrossRef](#)]
68. Yang, E.S.; Christopher, S.A.; Kondragunta, S.; Zhang, X. Use of hourly Geostationary Operational Environmental Satellite (GOES) fire emissions in a Community Multiscale Air Quality (CMAQ) model for improving surface particulate matter predictions. *J. Geophys. Res. Atmos.* **2011**, *116*, D04303–1–D04303–13. [[CrossRef](#)]
69. Kanda, I.; Basaldud, R.; Magaña, M.; Retama, A.; Kubo, R.; Wakamatsu, S. Comparison of Ozone Production Regimes between Two Mexican Cities: Guadalajara and Mexico City. *Atmosphere* **2016**, *7*, 91. [[CrossRef](#)]
70. de Meij, A.; Cuvelier, C.; Thunis, P.; Pisoni, E.; Bessagnet, B. Sensitivity of air quality model responses to emission changes: comparison of results based on four EU inventories through FAIRMODE benchmarking methodology. *Geosci. Model Dev.* **2024**, *17*, 587–606. [[CrossRef](#)]
71. Bessagnet, B.; Bossioli, E.; Cholakian, A.; Vivanco, M.G.; Cuvelier, K.; Theobald, M.R.; Gil, V.; Menut, L.; de Meij, A.; Pisoni, E.; et al. Impact of air quality model settings for the evaluation of emission reduction strategies to curb air pollution. *Environ. Res.* **2024**, *255*, 119112. [[CrossRef](#)] [[PubMed](#)]
72. Shi, L.; Zhu, A.; Huang, L.; Yaluk, E.; Gu, Y.; Wang, Y.; Wang, S.; Chan, A.; Li, L. Impact of the planetary boundary layer on air quality simulations over the Yangtze River Delta region, China. *Atmos. Environ.* **2021**, *263*, 118685. [[CrossRef](#)]
73. de Lange, A.; Naidoo, M.; Garland, R.M.; Dyson, L.L. The sensitivity of simulated surface-level pollution concentrations to WRF-ARW-model PBL parameterisation schemes over the Highveld of South Africa. *Atmos. Res.* **2021**, *254*, 105517. [[CrossRef](#)]
74. Wang, J.; Zhang, B.; Zhang, H.; Lv, M. The impacts of three PBL schemes on the simulation of boundary layer meteorological factors and air pollutants in Northern China. *IOP Conf. Ser. Earth Environ. Sci.* **2019**, *227*, 052011. [[CrossRef](#)]

75. Kurokawa, J.; Ohara, T. Long-term historical trends in air pollutant emissions in Asia: Regional Emission inventory in ASia (REAS) version 3. *Atmos. Chem. Phys.* **2020**, *20*, 12761–12793. [[CrossRef](#)]
76. Janssens-Maenhout, G.; Crippa, M.; Guizzardi, D.; Dentener, F.; Muntean, M.; Pouliot, G.; Keating, T.; Zhang, Q.; Kurokawa, J.; Wankmüller, R.; et al. HTAP_v2.2: A mosaic of regional and global emission grid maps for 2008 and 2010 to study hemispheric transport of air pollution. *Atmos. Chem. Phys.* **2015**, *15*, 11411–11432. [[CrossRef](#)]
77. Guenther, A.; Karl, T.; Harley, P.; Wiedinmyer, C.; Palmer, P.I.; Geron, C. Estimates of global terrestrial isoprene emissions using MEGAN (Model of Emissions of Gases and Aerosols from Nature). *Atmos. Chem. Phys.* **2006**, *6*, 3181–3210. [[CrossRef](#)]
78. Carn, S.; Fioletov, V.; McLinden, C.; Li, C.; Krotkov, N. A decade of global volcanic SO₂ emissions measured from space. *Sci. Rep.* **2017**, *7*, 44095. [[CrossRef](#)]
79. Cohan, D.S.; Napelenok, S.L. Air Quality Response Modeling for Decision Support. *Atmosphere* **2011**, *2*, 407–425. [[CrossRef](#)]
80. Kwok, R.; Napelenok, S.; Baker, K. Implementation and evaluation of PM_{2.5} source contribution analysis in a photochemical model. *Atmos. Environ.* **2013**, *80*, 398–407. [[CrossRef](#)]
81. Acid Deposition Monitoring Network in East Asia (EANET). *Data Report 2019*; Technical Report; Acid Deposition Monitoring Network in East Asia (EANET): Niigata, Japan, 2020.
82. Huang, L.; Zhu, Y.; Zhai, H.; Xue, S.; Zhu, T.; Shao, Y.; Liu, Z.; Emery, C.; Yarwood, G.; Wang, Y.; et al. Recommendations on benchmarks for numerical air quality model applications in China—Part 1: PM_{2.5} and chemical species. *Atmos. Chem. Phys.* **2021**, *21*, 2725–2743. [[CrossRef](#)]
83. Chuersuwan, N.; Nimrat, S.; Lekphet, S.; Kerdkumrai, T. Levels and major sources of PM_{2.5} and PM₁₀ in Bangkok Metropolitan Region. *Environ. Int.* **2008**, *34*, 671–677. [[CrossRef](#)] [[PubMed](#)]
84. Oanh, N.T.K. *Final Report on the Study of Sources of Particulate Matter Less Than 2.5 Microns (PM_{2.5}) and Secondary Pollutants (Secondary PM_{2.5}) in Bangkok and Surrounding Areas*; Technical Report; Asian Institute of Technology (AIT): Bangkok, Thailand, 2017.
85. Narita, D.; Oanh, N.T.K.; Sato, K.; Huo, M.; Permadi, D.A.; Chi, N.N.H.; Ratanajaratroj, T.; Pawarmart, I. Pollution Characteristics and Policy Actions on Fine Particulate Matter in a Growing Asian Economy: The Case of Bangkok Metropolitan Region. *Atmosphere* **2019**, *10*, 227. [[CrossRef](#)]

Disclaimer/Publisher's Note: The statements, opinions and data contained in all publications are solely those of the individual author(s) and contributor(s) and not of MDPI and/or the editor(s). MDPI and/or the editor(s) disclaim responsibility for any injury to people or property resulting from any ideas, methods, instructions or products referred to in the content.